Effect of temperature and heating rate on the sintering performance of SiC–Al 2 O 3 –Dy 2 O 3 and SiC–Al 2 O 3 –Yb 2 O 3…

Article *in* Ceramics International · September 2017

DOI: 10.1016/j.ceramint.2017.09.118

CITATIONS
0

READS
14

5 authors, including:

S. Ribeiro
University of São Paulo (USP) - Engineering S…
66 PUBLICATIONS **544** CITATIONS
SEE PROFILE

Luis A. Genova
Instituto de Pesquisas Energéticas e Nucleares
42 PUBLICATIONS **422** CITATIONS
SEE PROFILE

Giseli CRISTINA Ribeiro
Universidade Federal Fluminense
7 PUBLICATIONS **15** CITATIONS
SEE PROFILE

Ana Helena Bressiani
Instituto de Pesquisas Energéticas e Nucleares
172 PUBLICATIONS **1,014** CITATIONS
SEE PROFILE

Ceramics International 43 (2017) 16048–16054

Contents lists available at ScienceDirect

Ceramics International

journal homepage: www.elsevier.com/locate/ceramint

Review article

Effect of temperature and heating rate on the sintering performance of SiC-Al_2O_3-Dy_2O_3 and SiC-Al_2O_3-Yb_2O_3 systems

S. Ribeiro[a,*], L.A. Gênova[b], G.C. Ribeiro[a], M.R. Oliveira[a], A.H.A. Bressiani[b]

[a] Department of Materials Engineering (DEMAR), Lorena School of Engineering (EEL), University of São Paulo (USP), Estrada Santa Lucrecia s/n, Bairro Mondezir, CP 116, CEP 12600-970 Lorena, SP, Brazil

[b] Nuclear Energy Research Institute (IPEN), São Paulo, SP, Brazil

ARTICLE INFO

Keywords:
D. SiC
A. sintering
Shrinkage
Heating rate

ABSTRACT

Samples of SiC + 10 vol%($Al_2O_3 + Dy_2O_3$) and SiC + 10 vol%($Al_2O_3 + Yb_2O_3$) mixtures were obtained by cold isostatic pressing and sintered for one hour in a dilatometer at 1800 °C and 1900 °C, applying heating rates of 10, 20 and 30 °C/min. The results of the complete sintering cycle indicated that the heating rates do not significantly influence the shrinkage, but that temperature and total sintering time may be relevant factors. The compacts sintered at 1900 °C shrank on average 9% more than those sintered at 1800 °C, and it was found that the sintering time can be reduced by 40–50% at faster heating rates. The maximum shrinkage rates occurred at temperatures lower than those of the sintering thresholds for the two mixtures, two temperatures and three heating rates. It was also found that after formation of the liquid, the mechanisms of particle rearrangement and solution-precipitation were not as fast as reported in the literature, even at high heating rates, for example 30 °C/min, but they are responsible for much of the shrinkage occurring throughout the sintering cycle.

1. Introduction

Silicon carbide ceramics, which have been studied for many years, continue to stand out due to their properties, and hence, their applications [1–11]. Some important properties are high modulus of rupture, high hardiness, good corrosion resistance, high thermal conductivity, low density and thermal expansion, wear resistance and many others [1–4,6]. Due to these properties silicon carbide ceramics have many applications in the petroleum, chemical, automotive, aerospace and microelectronic industries [1], as diesel engine components, gas turbines, heat exchange [2], susceptors, heaters, and so on [3].

A common practice is liquid phase sintering (LPS) of silicon carbide ceramics, which not only promotes the formation of characteristic microstructures for various applications but is also faster and requires lower temperatures than solid phase sintering (SPS) [1–3,5,7–9].

Various additives can be used to promote liquid phase sintering of SiC, including the following oxides and mixtures of oxides: Al_2O_3, MgO, Y_2O_3, Al_2O_3-Y_2O_3, Al_2O_3-Y_2O_3-SiO_2, Y_2O_3-La_2O_3, Y_2O_3-Sc_2O_3, Al_2O_3-Dy_2O_3, and Al_2O_3-Yb_2O_3 [2,3,5–9].

LPS occurs in various stages as a function of time and temperature, i.e., formation and distribution of the liquid, wetting and rearrangement of solid particles under the influence of capillary forces, and solution-reprecipitation [2,12–14]. The stages of liquid formation and particle rearrangement are faster than that of solution-reprecipitation [12]. Incipient solid phase sintering may occurs prior to the formation of liquid, i.e., at lower temperatures and in shorter times, causing the compact to shrink slightly. If this occurs, the mechanisms at play are evaporation/condensation and surface diffusion [2,15,16].

Dilatometry can be used to investigate of the sintering process, enabling information about the thermal behavior of the material throughout the sintering cycle (heating, isotherm and cooling) to be obtained from a single sample. This information can be obtained based on the sample's dimensional variations over time, with a slight initial expansion, but with high shrinkage rates, particularly close to the threshold temperature [2,17–19].

Linear shrinkage as a function time or temperature curves are drawn based on the shrinkage measured in the dilatometer. These curves can be divided into four regions: linear expansion, shrinkage during non-isothermal heating, isothermal shrinkage, and cooling [20]. Specific events may appear as a function of reactions or transformations during sintering, in which case the curves will have more than four regions. In shrinkage vs. time curves, even the slightest changes are clearly visible. In this case, there is an instantaneous shrinkage rate curve, which is much more sensitive to minor changes compared to a shrinkage vs. time or temperature curve [15]. The shape, height, width and position of these shrinkage rate curves provide very important information for the

* Corresponding author.
E-mail address: sebastiao@demar.eel.usp.br (S. Ribeiro).

http://dx.doi.org/10.1016/j.ceramint.2017.09.118
Received 13 April 2017; Received in revised form 6 September 2017; Accepted 14 September 2017
Available online 18 September 2017

evaluation of sintering behavior. Long narrow curves suggest high shrinkage rates of the green body, while shorter wider curves suggest lower shrinkage rates [16,21].

The heating rate is a very important parameter in sintering, and several authors [2,15,16,18,19,22–24] have discussed its influence on the density and other properties of sintered materials. There are many controversies about shrinkage behavior and densification in response to heating rates. This subject is discussed in the literature [15,16,22–24], but it is worthwhile keeping in mind the following points:

1) Before the formation of liquid, shrinkage increases as the heating rate decreases.
2) At a given temperature, the shrinkage rate is lower at a lower heating rate, i.e., the peak of the shrinkage rate increases in height with the heating rate, contributing to rearrange the particles and increase densification.
3) The peak of the shrinkage rate indicates the separation of the solid-solid bonds by the liquid phase, and densification due to particle rearrangement.
4) The peak of the shrinkage rate increases along with the heating rate, indicating that the contribution of particle rearrangement to densification is greater at higher heating rates [15,16,22–24].

The main objective of this work was to study the sintering behavior of SiC with eutectic mixtures of Al_2O_3-Dy_2O_3 and Al_2O_3-Yb_2O_3 as a function of temperature and heating rate, using shrinkage as the parameter under study. Other objective of this study is to complement of our research group using the above cited additive systems to investigate the liquid-phase sintering of silicon carbide [25–27]

2. Materials and methods

The materials and experimental procedure adopted here were the same as those used in a previous study [2].

The samples were sintered under the following conditions: isothermal holding temperatures of 1800 and 1900 °C, for 1 h, at heating rates of 10, 20 and 30 °C/min., in order to compare the effect of these variables on the shrinkage. Table 1 describes the types and amounts of materials used in each mixture.

3. Results and discussion

For a better understanding of the results, Fig. 1 illustrates the main points discussed in this paper, using the SiCDy mixture sintered at 1800 °C with a 60 min isotherm and heating rate of 10 °C/min., as example. The points A, B, C, PMSR, D and E, shown in Fig. 1 are the same as those of the curves in Fig. 2, but respecting the slight differences, such as the displacement of points due to composition, sintering temperature and heating rate.

Fig. 1 shows all the curves of: (a) linear shrinkage ($\Delta L/L_0$) vs. temperature; (b) shrinkage vs. time; (c) shrinkage rate vs. time; and (d) a set of all the aforementioned curves shown in this paper.

Curves (a), (b) and (c) in Fig. 1 will be used concomitantly in the analysis of the behavior of the samples during sintering. The most important points on regions of the curves for this work are identified and discussed below.

Section 0 to A – Shows a slight linear expansion attributed to the natural thermal expansion of the components of the mixtures, up to about 1100–1200 °C.

Section A to B – Shows minor linear shrinkage at temperatures in the range of approximately 1100–1540 °C, which can be attributed to a small rearrangement of particles, reaction of the liquid phase forming additives, and incipient solid state sintering caused by slightly densifying mechanisms.

Section B to C – Onset of significant linear shrinkage caused by the formation of liquid and activation of the particle rearrangement mechanism.

Section C to D – The shrinkage vs. temperature curves show a marked drop, indicating very rapid shrinkage. As can be seen in Fig. 1(c), the highest shrinkage rate occurs in this section of the curve, i.e., the point of maximum shrinkage rate (PMSR). This rapid shrinkage can be attributed to the mechanisms of particle rearrangement and solution-reprecipitation, a common phenomenon in liquid phase sintering of covalent ceramics. Probably the solution-reprecipitation mechanism starts before of the end of rearrangement mechanism, an overlap of the different mechanism may occur. A short peak has been observed, see point "C", which may indicate the end of the particle rearrangement [10], however in the others time versus shrinkage rate curves, Fig. 2(e, f, g, and h) this event does not occur.

Section D to E – The shrinkage rate decreases considerably, reaching a value close to zero. Shrinkage continues, albeit slowly. This section of the curve contains the isothermal period of sintering, followed by the cooling up to the end of curves 1(a) and 1(b).

Fig. 1(b) illustrates the behavior of linear shrinkage as a function of time along the entire sintering cycle. The points indicated in this figure are the same as those indicated in Fig. 1(a), for comparison. The temperatures indicated here are approximations that mark the beginning or end of interesting phenomena to explain the liquid phase sintering of SiC.

Plotting the first derivative of the curve indicated in Fig. 1(b) results in the curve shown in Fig. 1(c), which represents the shrinkage rate, d ($\Delta L/L_0$), vs. time, showing details that are more difficult to observe as in Fig. 1(a) and (b). A series of small peaks are visible in the region inside the circle in Fig. 1(c), which, albeit very small, have a physical and phenomenological significance in sintering. After the region pointed out in the circle, the shrinkage rate increases sharply up to the PMSR, which is caused by the mechanisms of particle rearrangement and solution-reprecipitation. After reaching the PMSR, the shrinkage rate decreases very quickly up to point D, but with less intensity than between points C and the PMSR. After point D, the shrinkage rate decreases with less intensity until it reaches a value close to zero, at point E, indicating that the shrinkage continues but at a nearly constant speed and much more slowly than before, until the sintering cycle is completed.

In Fig. 1(c), note that there are two perfectly straight lines between points C and the PMSR, and between the PMSR and D, and in this case it is possible to determine the time period in which the highest shrinkage rates occurs, i.e., the time elapsed between points C and D.

The curve in Fig. 1(d) represents the complete set of curves of shrinkage vs. time and temperature, and shrinkage rate and temperature vs. time. This set of curves makes it very easy to evaluate the shrinkage and shrinkage rate as a function of time and temperature throughout the entire sintering cycle.

Based on this preliminary information, the results are shown and discussed considering the effect of heating rate and temperature on shrinkage and on the shrinkage rate during the complete sintering cycle, and also specifically during the heating ramp.

Fig. 2 shows the curves created from the data obtained from the tests performed in the dilatometer, (a), (b), (c) and (d), as well as their respective derivatives, (e), (f), (g) and (h). The curves of (a) to (d)

Table 1
Composition of the SiC, Al_2O_3, Dy_2O_3 and Yb_2O_3 mixtures.

Powder mixtures	Code	Components (wt) (wt%)			
		SiC	Al_2O_3	Dy_2O_3	Yb_2O_3
SiC + 10 vol% (Al_2O_3 + Dy_2O_3)	SiCDy	120 g	12.10 g	8.45 g	0.00
		85.38%	8.61%	6.01%	0.00
SiC + 10 vol% (Al_2O_3 + Yb_2O_3)	SiCYb	120 g	12.76 g	0.00	9.39 g
		84.42%	8.98%	0.00	6.60%

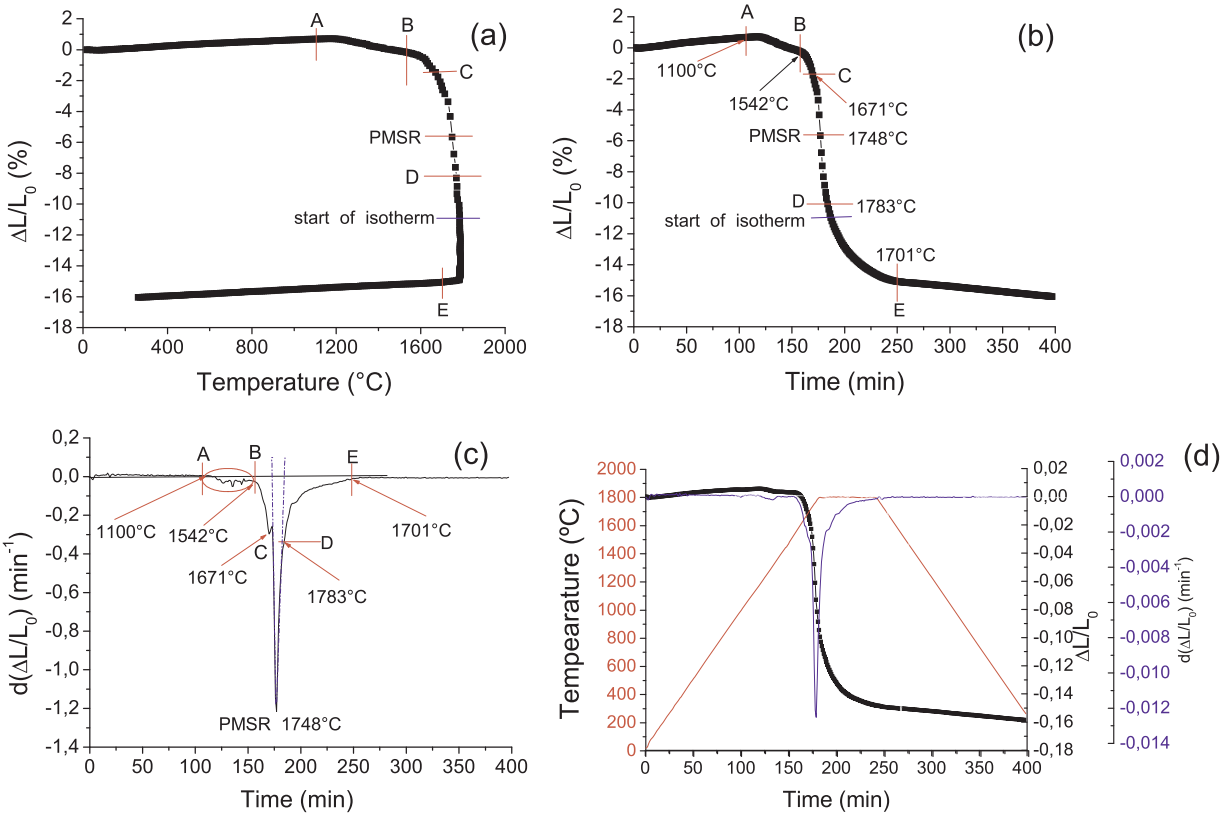

Fig. 1. (a) Shrinkage vs. temperature; (b) shrinkage vs. time; (c) shrinkage rate vs. time; (d) shrinkage vs. time and temperature, and shrinkage rate vs. time and temperature.

illustrate the behavior of linear shrinkage, S, of the SiCDy and SiCYb samples as a function of temperature and heating rate for the complete sintering cycle.

The two compositions show very similar shrinkage vs. temperature curves at the two temperatures and at the three heating rates. This enables one to draw a master sintering curve, which is widely studied in this field of science and technology [19,22,24], but is outside the scope of this study.

A comparison of the values of linear shrinkage, S, listed inside the graphs in Fig. 2 revealed that the samples of both compositions sintered at 1900 °C shrank a little more than those sintered at 1800 °C. Also, note that there is a slight separation of the curves of the samples at sintered 1900 °C in the region of high shrinkage compared to those sintered at 1800 °C. However, this small difference does not lead to very different results, especially when one considers the total sintering cycle. These shrinkage are comparatively higher than those reported in previous studies, which used SiC with mixtures of aluminum oxides and rare earths [10,11].

In Fig. 2, curves (e), (f), (g) and (h) were drawn from the derivative of curves (a), (b), (c) and (d), respectively, which clearly show the kinetics of shrinkage of the two compositions at the three heating rates. The internal legends of the graphs in Figs. 2(e) to 2(h) indicate the temperatures of maximum shrinkage rates (TMSR) and their respective values (SR). All the points of maximum shrinkage rates (PMSR) occurred while still in the heating stage of the sintering, slightly before the isotherm. This means that much of the shrinkage, and hence of densification, occurs while the material is still in the heating stage of the sintering cycle, see results presented in Fig. 3(a-d), as indicated by S_{rel}(%).

As can be seen in the shrinkage vs. time curves, several small peaks appear at times and hence temperatures prior to the onset of rapid shrinkage (see the region inside the circle in Fig. 1(c)), which indicate the occurrence of events whose effect on shrinkage is negligible. Formation of liquid occurs immediately after these events (see point B in Fig. 1(a), (b) and (c)) and, at this point, shrinkage develops at high rates. This can be observed in the shape of the curves, since narrower curves suggest high shrinkage rates of the green compact [21].

An evaluation of the maximum shrinkage rates, SR, indicates that only the heating rate of 10 °C/min resulted in lower shrinkage rates than those obtained at the heating rates of 20 and 30 °C/min, which were similar to each other. The curves corresponding to the heating rate of 10 °C/min for both compositions and temperatures are less intense and more open that those corresponding to the heating rates of 20 and 30 °C/min, which are more intense and narrower. Results similar to these are reported quite frequently in the literature on sintering of other ceramic materials [15,16,21–24].

The information in Table 2 is based on an evaluation of the time spent by the two compositions in the region of fast shrinkage, i.e., between points C-PMSR-D, shown in Fig. 1(c), but also for Fig. 2, at the three heating rates.

Table 2 shows minor differences in the time elapsed for the maximum shrinkage rates to occur; these slight differences tend to become even smaller at higher heating rates.

Another important observation is that, after passing through the region demarcated by the circle, on the right side of the curves, the curves assume a unimodal shape with very well defined lines. This suggests that the formation of liquid, and hence, particle accommodation and the solution-precipitation process, occur in a harmonious sequence over time; otherwise, these curves would be marked by more than one peak of maximum shrinkage speed, i.e., more than one mode.

The height, position, and width of the peaks of shrinkage rate vs. time are indicative of the activation energy of shrinkage mechanisms, and hence, of densification [24]. As for the width and height of the peaks in the shrinkage rate vs. time curves, Fig. 2, the curves corresponding to the heating rate of 10 °C/min are less intense for the two mixtures and at the two temperatures, with lower values of maximum shrinkage rate, SR, and wider than those at 20 and 30 °C/min. The reason for this behavior may be linked to incipient solid state sintering,

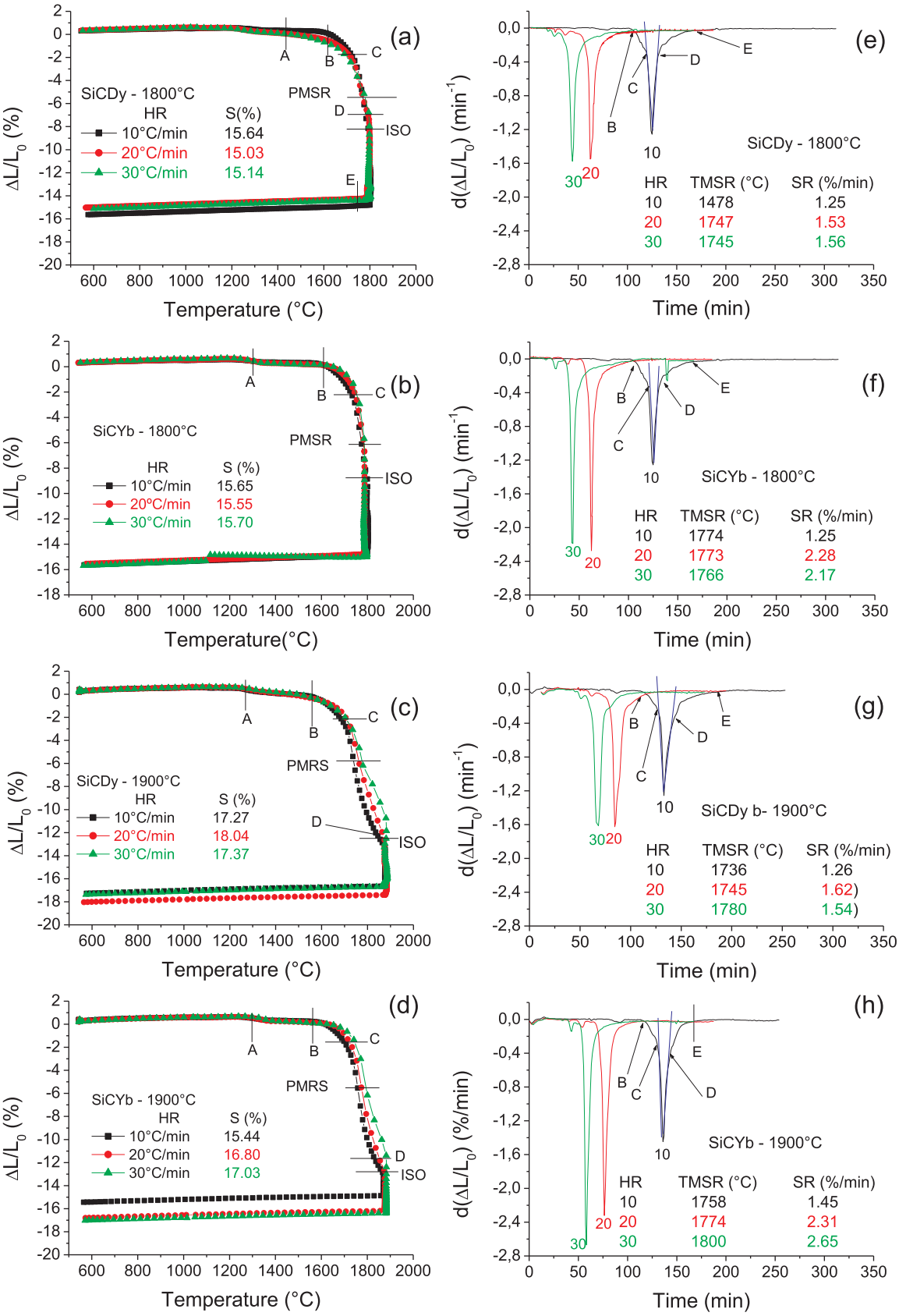

Fig. 2. Dilatometer curves of the mixtures of SiCDy: (a) and (c); and SiCYb: (b) and (d), as well as their respective derivatives (e), (f), (g) and (h), sintered at 1800 °C and 1900 °C, applying heating rates of 10, 20 and 30 °C/min in the complete sintering cycle. S: total Shrinkage; HR: Heating Rate; TMSR: Temperature of Maximum Shrinkage Rate; SR: Shrinkage Rate (measured at the PMSR).

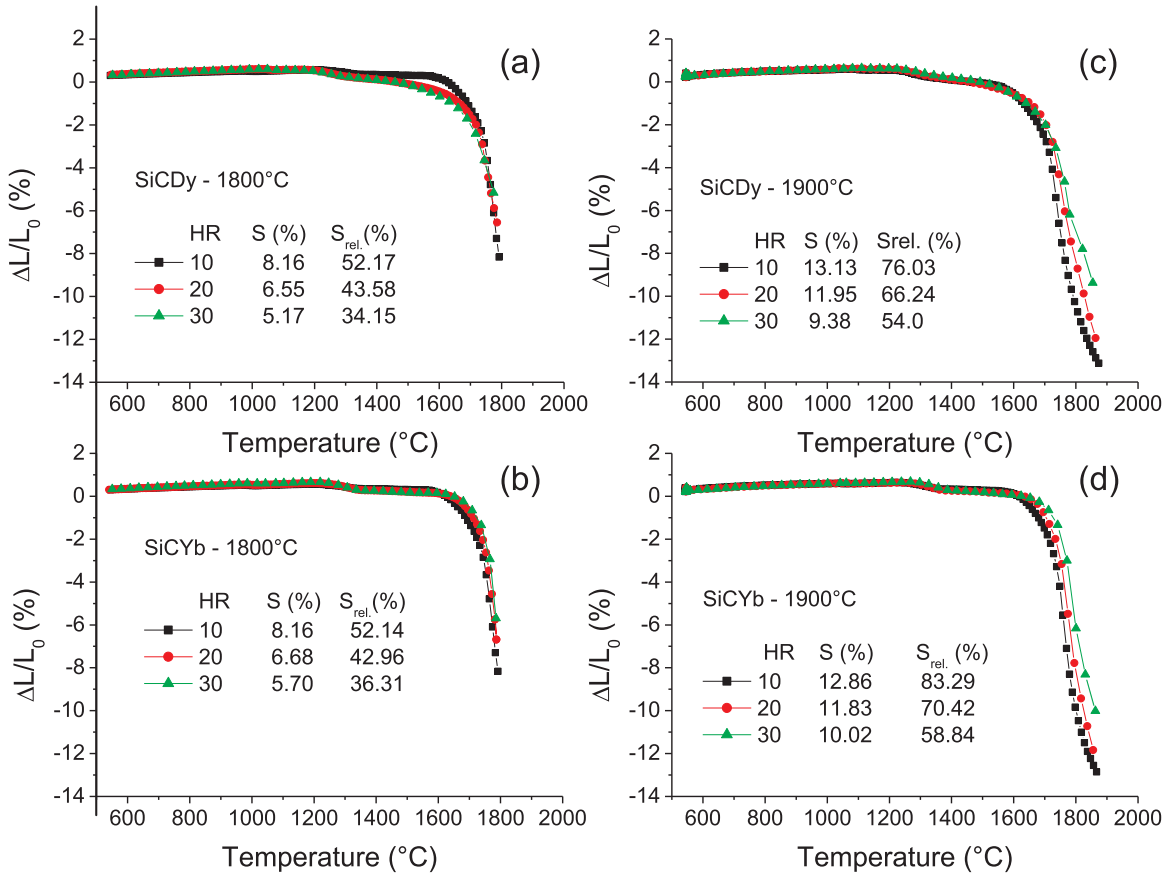

Fig. 3. Dilatometer curves of the heating step of the SiCDy: (a) and (c), and SiCYb: (b) and (d) mixtures, sintered under non-isothermal conditions up to 1800 °C, (a) and (b), and 1900 °C, (c) and (d), at heating rates of 10, 20 and 30 °C/min. $S_{rel.}$: relative Shrinkage.

Table 2
Time elapsed for the fastest SiC sintering step to be achieved with the respective additives, in each situation, taking Fig. 1(c) as an example.

Heating rate	SiCDy		SiCYb	
	1800 °C	1900 °C	1800 °C	1900 °C
10 °C/min	15 min	16 min	16 min	14 min
20 °C/min	13 min	14 min	12 min	13 min
30 °C/min	12 min	13 min	11 min	11 min

since the components of the compositions take relatively longer to reach the liquid forming temperature in the system, and this promotes a difference in the energy stored in the compact for the same temperature.

The influence of the intensity of the maximum shrinkage rate (SR) as a function of the rate of shrinkage has been exhaustively discussed in previous studies [15,16,22–24]. Those studies contain contradictory data, but most of them have found higher shrinkage rates at the PMSR occur at higher heating rates. This finding is in agreement with the present work, where a difference was found, especially compared with the heating rates of 10 °C/min and 20 °C/min. The difference in shrinkage rates between the heating rates of 20 and 30 °C/min was negligible.

In addition to the results shown in this paper, other benefits can be achieved at higher heating rates, such as smaller grain sizes, as reported by Ribeiro et al. [2]. Obviously the sintering time also decreases, representing savings in ceramics processing. In the case of this work, heating rates of 20 and 30 °C/min resulted in a 40–50% decrease in sintering time compared to that required at the heating rate of 10 °C/min, without a significant loss through shrinkage.

Table 3
Influence of the heating rate in the sintered density, shrinkage and weight loss for samples SiCDy and SiCYb sintered at 1800 °C.

Code	Heating rate (°C/min)	Green density (%)	Sintered density (%)	Shrinkage (%)	Weight loss (%)
SiCDy	10	52.40	92.25	15.64	12.07
	20	52.45	91.33	15.03	11.61
	30	52.42	90.88	15.14	11.10
SiCYb	10	53.64	92.01	15.65	13.05
	20	53.56	91.15	15.55	13.10
	30	53.66	91.16	15.70	13.03

Table 4
Influence of the heating rate in the sintered density, shrinkage and weight loss for samples SiCDy and SiCYb sintered at 1900 °C.

Code	Heating rate (°C/min)	Green density (%)	Sintered density (%)	Shrinkage (%)	Weight loss (%)
SiCDy	10	52.41	93.18	17.27	13.01
	20	52.46	93.05	18.04	12.98
	30	52.38	92.96	17.37	12.90
SiCYb	10	52.86	93.01	15.44	13.01
	20	52.96	93.00	16.80	12.93
	30	52.91	93.08	17.03	12.86

In order to complete the sintering study, considering the complete sintering cycle, of the SiC mixtures plus additives, the samples after sintering were characterized by their green density, sintered density, shrinkage and weight loss. The results are shown in Tables 3 and 4. It can be observed that density of the samples followed the same behavior of the shrinkage, that is, small differences among SiDy samples sintered

with heating rates of 10, 20 or 30 °C/min., for both maximum temperatures. For the SiCYb composition the difference of densities due to different heating rates are very small. In all cases the densities of samples sintered with 10 °C/min presented superior density than samples sintered with higher heating rates, 20 or 30 °C/min. It can also be observed that the change in sintering temperature from 1880 °C to 1900 °C increased the final density, on average, only 2%. The density of the sintered samples seems to be low and their mass loss high, but one has to consider that these results were obtained by sintering in a dilatometer under argon flux. Obviously, these results are improved when the sintering is carried out in a controlled static atmosphere and using the powder bed technique [10].

Fig. 3 illustrates shrinkage vs. temperature curves for the SiCDy and SiCYb compositions during the heating step, i.e., before reaching the 1800 and 1900 °C isotherms, respectively. Note that in this sintering stage, the heating rate has a significant effect on the linear shrinkage of the samples, showing decreasing values in response to the increase in the heating rate applied to the two compositions. The graphs in Fig. 3 show the values of linear shrinkage, S, and relative shrinkage, S_{rel}, where S_{rel} was calculated from the linear shrinkage, S, depicted in Fig. 3(a–d), divided by the total linear shrinkage, S, depicted in Fig. 2(a–d), respectively.

An analysis solely of the effects of the heating step, before the isotherm, indicated that the heating rate interfered significantly in the shrinkage of the samples of both compositions at the two non-isothermal sintering temperatures. Moreover, an analysis of the influence of the heating rate on the two compositions revealed that at both 1800 °C and 1900 °C, lower heating rates promoted higher shrinkage, S, which varied from 34% to 83%. This was already expected, since lower heating rates lead to longer retention times of samples in the kiln, and hence, higher shrinkage. These results are in agreement with most of the articles available in the literature about the influence of heating rates on the shrinkage of ceramics, although there are controversies [15,16,22–24].

Temperature also strongly affects shrinkage during the heating of samples. The shrinkage of samples differed significantly when heated to 1800 °C and 1900 °C, at the same heating rates (see graphs and legends of curves (a) and (c), (b) and (d) in Fig. 3). In the SiCDy composition, these differences varied from 52% to 76%, from 44% to 66%, and from 34% to 54% in response to heating rates of 10, 20 and 30 °C/min, respectively. These heating rates also caused variations in the shrinkage of the SiCYb composition, ranging from 52% to 83%, from 43% to 70% and from 36% to 59%. Higher temperatures obviously result in greater shrinkage, not to mention the additional sintering time caused by increasing the temperature from 1800 °C to 1900 °C.

Shrinkage was also noticeably influenced by the composition of the mixture, considering the heating period, since the SiCYb samples showed greater shrinkage than the SiCDy samples at 1900 °C, although this was not observed at 1800 °C. However, it is interesting to note that this difference in shrinkage during the heating stage does not apply when one considers the complete sintering cycle, and that this behavior is rarely discussed in papers on ceramics sintering, particularly when it comes to SiC ceramics. A careful evaluation of these results and observations may be helpful in more effective planning of sintering, not only of SiC but also of ceramics in general.

The final shrinkage values were not significantly affected by the different heating rates, but the increase of 100 °C in the sintering temperature resulted in a slight increase in shrinkage of SiCDy and SiCYb samples at the three heating rates. This finding is in accordance with the theory, because at higher temperatures, the viscosity of liquid decreases and the diffusion processes increase in this phase, resulting in increased shrinkage.

An analysis of the temperatures of maximum shrinkage rate, TMSRs, revealed that neither the heating rate nor the sintering temperature exerted a significant influence, since the values were very close at the operating conditions adopted here. However, the TMSRs of the SiCDy composition were lower than those of the SiCYb composition. This fact may be attributed to the properties of the liquids formed by the different rare earth oxides. It was also found that as soon as the liquid was formed, the shrinkage rate increased very rapidly, and this is closely linked to the fact that the liquid causes wetting and rearrangement of the particles, followed immediately by the solution-precipitation process.

4. Conclusions

Checking the shrinkage vs. time or temperature curves obtained in the dilatometer during the complete sintering cycle provides only general information about shrinkage at any temperatures and heating rates. A good option to check shrinkage behavior during sintering is to elaborate partial shrinkage vs. time or temperature curves, which permits to observe effects that an analysis of the curve of the complete cycle does not reveal.

Higher heating rates generates taller and narrower shrinkage peaks than lower rates with significantly reducing the sintering time. The heating rate strongly affects the stages prior to the isotherm, a fact that deserves a more in-depth study to generate knowledge for the creation of sintering curves of ceramic materials.

The experience and results described here can be used to optimize the sintering process not only of SiC but also of other ceramics.

Acknowledgments

The authors gratefully acknowledge the support received from the São Paulo Research Foundation (FAPESP, Process nos. 2010/51925-6 and 2013/08032-9) and Brazil's National Council for Scientific and Technological Development (CNPq, Process n° 303061/2009-0 and 307432/2013-0), in the form of research productivity grants.

References

[1] K. Gan, J. Xu, X. Zhang, W. Huo, J. Yang, Preparation of silicon carbide ceramics using chemical treated powder by DCC via dispersant reaction and liquid phase sintering, J. Eur. Ceram. Soc. 37 (2017) 891–897.
[2] S. Ribeiro, L.A. Genova, G.C. Ribeiro, M.R. Oliveira, A.H.A. Bressiani, Effect of heating rate on the shrinkage and microstructure of liquid phase sintered SiC ceramics, Ceram. Int. 42 (2016) 17398–17404.
[3] T.-Y. Cho, Y.-W. Kim, K.J. Kim, Thermal, electrical, and mechanical properties of pressureless sintered silicon carbide ceramics with ytria-scandia-aluminum nitride, J. Eur. Ceram. Soc. 36 (2016) 2659–2665.
[4] G. Magnani, A. Brentari, E. Burresi, G. Raiteri, Pressureless sintered silicone carbide with enhanced mechanical properties obtained by the two-step sintering method, Ceram. Int. 40 (2014) 1759–1763.
[5] C.Y. Liu, W.-H. Tuan, S.C. Chen, Ballistic performance of liquid-phase sintered silicon carbide, Ceram. Int. 39 (2013) 8253–8259.
[6] A. Noviyanto, D.H. Yoon, Rare-earth oxide additives for the sintering of silicon carbide, Diam. Relat. Mater. 38 (2013) 124–130.
[7] E. Sánchez-González, P. Miranda, F. Guiberteau, A. Pajares, Effect of microstructure on the mechanical properties of liquid-phase-sintered silicon carbide at pre-creep temperature, J. Eur. Ceram. Soc. 31 (2011) 1131–1139.
[8] A. Can, M. Herrmann, D.S. McLachlan, I. Sigalas, J. Adler, Densification of liquid phase silicon carbide, J. Eur. Ceram. Soc. 26 (2006) 1707–1713.
[9] K. Biswas, G. Rixecker, F. Aldinger, Gas pressure of SiC sintered with rare-earth-(III)-oxides and their mechanical properties, Ceram. Int. 31 (2005) 703–711.
[10] J. Marchi, J.C. Bressiani, A.H.A. Bressiani, Densification studies of silicon carbide-based ceramics with ytria, silica and alumina as sintering additives, Mater. Res. 4 (2001) 231–236.
[11] J. Marchi, J.C. Bressiani, A.H.A. Bressiani, Dilatometric studies of (SiO_2-RE_2O_3-Al_2O_3) silicon carbide ceramic, Mater. Res. 8 (2005) 201–2015.
[12] M.N. Rahaman, Ceramic Processing, Taylor & Francis Group, Boken Sound Parkway NW, 2007.
[13] P.M. Ossi, R. Roberti, G. Silva, On the rearrangement mechanism during liquid phase sintering of a model system, Scr. Metall. 19 (1985) (1985) 569–574.
[14] T.H. Courtney, Densification and structural development in liquid phase sintering, Metall. Trans. A Phys. Metall. Mater. Sci. 15A (1984) 1065–1074.
[15] R. Bollina, R.M. German, Heating rate effects on microstructural properties of liquid phase sintered tungsten heavy alloys, Int. J. Refract. Met. Hard Mater. 22 (2004) 117–127.
[16] S.S. Ryu, Y.D. Kim, I.H. Moon, Dilatometric analysis on the sintering behavior of nanocrystalline W-Cu prepared by mechanical alloying, J. Alloy. Compd. 335 (2002) 233–240.

[17] B. Desplanques, F. Valdivieso, S. Saunier, Influence of processing parameters on the behaviour of thick bilayers (Cer/Cer) performed by powder processing: dilatometry without contact, Ceram. Int. 40 (2015) 15215–15225.
[18] A. Karamanov, B. Dzhantov, M. Paganelli, D. Sighinolfi, Glass transition temperature and activation energy of sintering by optical dilatometry, Thermochim. Acta 553 (2013) 1–7.
[19] D. Li, S. Chen, W. Shao, X. Ge, Y. Zhang, S. Zhang, Densification evolution of TiO_2 ceramics during sintering based on the master sintering curve theory, Mater. Lett. 62 (2008) 849–851.
[20] B.B. Panigrahi, M.M. Godkhindi, Dilatometric sintering study of Ti-50Ni elemental powders, Intermetallics 14 (2006) 130–135.
[21] E.A. Trusova, A.A. Khrushcheva, K.V. Vokhmintcev, D.D. Titov, Dilatometric sintering study of fine-grained ceramics from ultradispersed admixture composed of $Ce_{0,09}Zr_{0,91}O_2$ and MgO-Al_2O_3, J. Eur. Ceram. Soc. 33 (2013) 2327–2333.
[22] M. Mazaheri, A. Simchi, M. Dourandish, F. Golestani-Fard, Master sintering curves of a nanoscale 3Y-TZP powder compacts, Ceram. Int. 35 (2009) 547–554.
[23] H. Yhua, J. Donggliang, Z. Jingxian, C. Zhongmin, L. Qinggling, H. Zhengren, Sintering kinectics of YAG ceramics, J. Rare Earth 32 (2014) 416–422.
[24] K. Rajeswari, S. Padhi, A.R.S. Reddy, R. Johnson, D. Das, Studies on sintering kinetics and correlation with the sinterability of 8Y zirconia ceramics based on the dilatometric shrinkage curves, Ceram. Int. 39 (2013) 4985–4990.
[25] J.A. Silva, B.M. Moreschi, G.C.R. Garcia, S. Ribeiro, Wettability of silicon carbide ceramic by Al_2O_3/Dy_2O_3 and Al_2O_3/Yb_2O_3 systems, J. Rare Earth 31 (2013) 634–638.
[26] S. Ribeiro, G. Ribeiro, M.R. Oliveira, Properties of SiC ceramics sintered via liquid phase using Al_2O_3 + Y_2 O_3, Al_2 O_3 + Yb_2O_3 and Al_2O_3 + Dy_2O_3 as additives: a comparative study, Mater. Res. 18 (2015) 525–529.
[27] A.C. Santos, A.P. Luz, S. Ribeiro, Melting temperature and wetting angle of AlN/Dy_2O_3 and AlN/Yb_2O_3 mixtures on SiC substrates, Mater. Res. 18 (2015) 957–962.